NOVEMBER 01 1992

Observations of the oscillation modes of choked circular jets

Alan Powell; Yoshikuni Umeda; Ryuji Ishii

J. Acoust. Soc. Am. 92, 2823–2836 (1992)
https://doi.org/10.1121/1.404398

Observations of the oscillation modes of choked circular jets

Alan Powell
Department of Mechanical Engineering, University of Houston, Houston, Texas 77204-4792

Yoshikuni Umeda and Ryuji Ishii
Department of Aeronautical Engineering, Kyoto University, Kyoto 606, Japan

(Received 2 August 1991; revised 17 June 1992; accepted 30 July 1992)

Under-expanded jets exhausting from convergent circular nozzles are known to emit a powerful acoustic tone called *screech*. The steady decrease of the screech frequency with increasing pressure ratio is interrupted by four frequency jumps as the mode of jet instability changes successively from an axially symmetric (varicose, torroidal) one labeled A_1 (varicose, torroidal), to another but similar one labeled A_2, a sinuous (lateral, flapping) one B, a helical one C, and finally one that is identified here as a sinuous one, D. Digital FFT analyses disclose the simultaneous presence of *associated secondary* tones about 25 dB weaker than the dominant ones, the frequency of these secondary tones forming smooth continuations of the dominant tones. As a secondary tone connects the dominant B and D modes, it is inferred that these are actually the same mode interrupted by the helical mode C. However, their detailed behavior is significantly different: the plane of oscillation of B appears to have a preferred orientation but is accompanied by rather random oscillations in other planes, occasionally having a helical appearance, while D appears be in a single plane that rotates relatively slowly and unsteadily about the jet axis. The helical mode C appears very stable: its frequency is significantly higher ($\approx$14%–23%) than that of the adjacent sinuous mode(s). The convection velocity of the unstable waves in the jet varies from about 0.6 of the ambient sound speed for the modes A to the maximum of about 0.8 for mode B, these corresponding to about 0.6 of the fully expanded jet exit velocity.

PACS numbers: 43.28.Ra, 43.50.Nm, 43.28.Py

INTRODUCTION

The acoustic emission from a supersonic jet generally has a frequency spectrum that contains powerful discrete tones that have been called *screech*. First reported in 1951 (Powell, 1951) initial investigations concerned the screech of rectangular jets (Powell, 1953a) and certain common features with the classic phenomenon of edge tones were pointed out (Powell, 1953b). It was suggested that the radiated acoustic pressure acting on the jet at the nozzle exit changed the angle at which the supersonic jet boundary separated from the nozzle edge, and so excited sinuous modes of the jet. These instability waves grew in amplitude as they were convected downstream because of their intrinsic instability and interacted with the periodic structure of the under-expanded jet to produce an array of stationary acoustic sources. Two criteria were developed that govern the existence of sustained oscillations of the feedback loop (see also Powell, 1953c). A phase relationship concerned the wavelengths involved and the geometrical size of the feedback loop. An amplitude criterion concerned the gain around the feedback circuit; this involved the amplification of the sinuous disturbance of the jet and also the effectiveness by which the stationary sources radiated back to the nozzle. The latter is quite frequency dependent, and, given that the frequency lies in the broader range of frequencies where the jet has a high degree of instability, it was hypothesized that the frequency should be such that the directionality of the array is maximized in the direction of the nozzle. This last criterion is the same as requiring that the periodic waves from each of the sources in the array should arrive at the nozzle with the same phase so as to produce the maximum disturbance of the jet flow there (Powell, 1953b, 1953c, 1962; see also Tam *et al.*, 1986; Tam, 1988). In the two-dimensional case the screech frequency decreases smoothly as the jet pressure ratio increases, the acoustic wavelength increasing as the periodic cell length of the jet lengthens with increasing pressure ratio. There is good agreement between calculated frequencies and those observed (Powell, 1953a; Tam, 1988)

In the case of the jet issuing from a convergent circular nozzle the downwards trend of the frequency was found to be interrupted by jumps in frequency (Powell, 1953c). The frequencies—*when steady enough*—were determined, very precisely, by matching the signal from a microphone (or from a photomultiplier with a schlieren pin-hole) with that of an oscillator. Following the edge tone convention, each of the regions where the frequency varied smoothly was called a *stage*, and were labeled A, B, C, and D (for a reason to appear shortly, these are now capitalized). The frequency at which the jump from stage C to stage D occurred as the pressure increased was different to that at which the jump from D to C occurred as the pressure decreased, i.e., a hysteretic effect was present. This was the only hysteretic jump observed.

 0001-4966/92/112823-14$00.80

So far as the unstable motion of the jet was concerned, schlieren photographs showed a toroidal mode of instability of the jet during stage A. The photographs for the other stages all had an asymmetric appearance, so they were either sinuous (lateral) or helical, but at the time it was not possible to distinguish between such modes.

Using high-speed stroboscopic lighting, Merle (1956) found the same staging structure of the frequency for the screech from circular jets, except that there were two separate but similar parts to stage A, which we now label A_1 and A_2. Pertinent to the present study, she simply noted, without further comment, that the stage A_1 was unstable, A_2 stable, B very unstable, C very stable, and finally stage D was unstable and not always visible. She also noted, very briefly and also without comment, the existence of weak periodicities that had the appearance of continuations of the labeled stages.

In later investigations, Davies and Oldfield (1962) employed two microphones, the signals from which formed Lissajous figures on an oscilloscope and in this way they established that both the A stages had axially symmetric acoustic fields, implying that the responsible instability modes of the jet were likewise axisymmetric (toroidal or varicose, to use Rayleigh's term). They also determined that for stage B the pair of microphones had signals that were either in phase or out of phase with each other, i.e., the responsible instability wave of the jet must be sinuous in a plane. The systematic change in the Lissajous figure with angular microphone separation led to the conclusion that stage C was helical in structure.

The helical mode has since been confirmed by near-field pressure measurements by Westley and Wooley (1975), who studied the expanding helical sound field in some detail. More recently, Gutmark *et al.* (1989) reported the existence of varicose and helical modes only, although there seems some possibility that sinuous modes might have occurred, since it appears that the technique employed would not be able to provide discrimination between sinuous and helical modes. The foregoing studies involved convergent nozzles only. Yu and Seiner (1983) studied the helical mode in the jet issuing from a convergent-divergent nozzle with the design exit Mach number of 2.0, operating at pressure ratios different from the design value. However, mode D of the simple choked jet has resisted classification by the methods employed so far, although it was suggested that the intermittency which had been observed, at a frequency of a few cycles per second, might have been due to the plane of the sinuous motion rotating about the jet axis due to a slight swirl in the flow (Powell, 1953c). This point is investigated in some detail in the present work.

Now the term "stage" was coined with reference to the low-speed edge tone: the instability mode of the jet in this case is invariably sinuous, and the numbered stages are related to the number of cycles in the feedback loop. The situation here is really quite different: the instability *mode* of the jet changes—varicose, sinuous, or helical. Thus these will be henceforth labeled *modes*, while mode A has two *stages*, A_1 and A_2.

The present work covers the same ground as did the initial study of circular jet screech (Powell, 1953c), but exploits modern instrumentation to extract new information. The frequency characteristics are defined using digital analyzers, schlieren photographs make visible the jet instability modes and the associated sound fields (if strong enough), while the digital equipment makes possible detailed studies of the correlation and phase relationships in the sound field around the jet.

I. EXPERIMENTAL APPARATUS

The convergent circular nozzle of these studies had an exit internal diameter of $d = 10$ mm, preceded by a short parallel section connecting to a 16° half-angle conical section, see Fig. 1. The maximum pressure ratio attainable with this circular nozzle was 5.84. The total contraction (area) ratio was 100:1. The external diameter in the exit plane was 26 mm, i.e., the "lip" of the nozzle was 8 mm thick, almost equal to the exit diameter. [The "lip," which has some importance in determining the strength of the feedback cycle, in Powell's original work was one half of the exit diameter thick (diameter 25.4 mm), those in Davies and Oldfield's experiments were unstated but apparently much thinner and those in Merle's case much thicker, about 2.5 diameters.] No sound absorption material or angled reflector was applied to this thick lip. For a secondary experiment used to validate some of the correlation work a convergent rectangular nozzle with internal exit dimensions of $b = 40$ mm by $a = 5$ mm was used.

The positions of the microphones used are also shown in Fig. 1. The radial distance r of the microphones from the jet axis was set at 77 mm. One microphone M_f was kept at a fixed position, while the other one, M_m, was rotated through the angle θ in steps of 15° about the axis, both microphones being kept in the plane at a fixed distance $s = 40$ mm upstream of the face of the nozzle. The fixed microphone M_f was a 6.4-mm-diam Brüel & Kjær type 4135 condenser microphone, and the moveable one was a B & K type 4138, 3.2 mm in diameter.

The signal outputs from the microphones were recorded on a TEAC R-410 data recorder, with direct mode recording

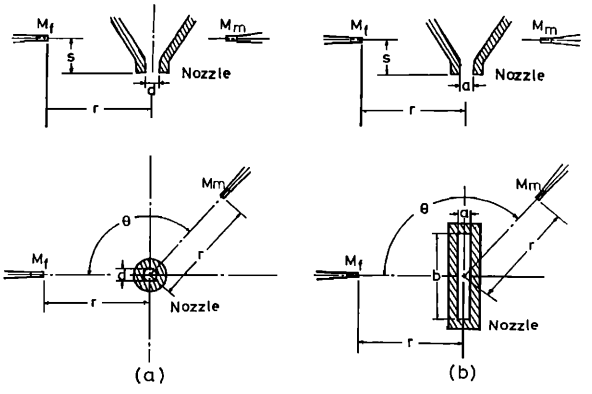

FIG. 1. Position of the fixed and moveable microphones, M_f and M_m, respectively, relative to circular and rectangular nozzles.

in the frequency band 100 Hz to 100 kHz. The data were analyzed using either the Fujitsu M 780-30 main frame computer in the Data Processing Center of Kyoto University or a TEAC C-120 digital correlator and an Ono Sokki CF 300 FFT digital frequency analyzer.

The jet was systematically turned off between the taking of each data sample for varying microphone separation angles and for different pressure ratios of the jet and between the taking of each photograph (except when investigating hysteretic characteristics).

The photographs were taken using a conventional single pass schlieren system, using 20-cm-diam mirrors of 200-cm focal length, with a Sugawara type MS-230 spark light source of duration about 1 μs. This system had been found to be highly satisfactory in previous work (Umeda *et al.*, 1987a).

II. EXPERIMENTAL RESULTS

A. Spectral analyses

First the frequency characteristics of the screech tones emitted by the circular choked jet at various pressure ratios R from 2.0 to 5.84 were determined. These pressure ratios correspond to the common measure of ideally fully expanded jet Mach numbers of 1.05 and 1.81, respectively. Figure 2 shows the results obtained.

The open circles indicate *dominant* tones, defined here as those that exceed the local broad band noise by at least 10 dB, usually by more than 30 dB. The five continuous segments are labeled in turn with capital letters, A_1, A_2, B, C, and D.

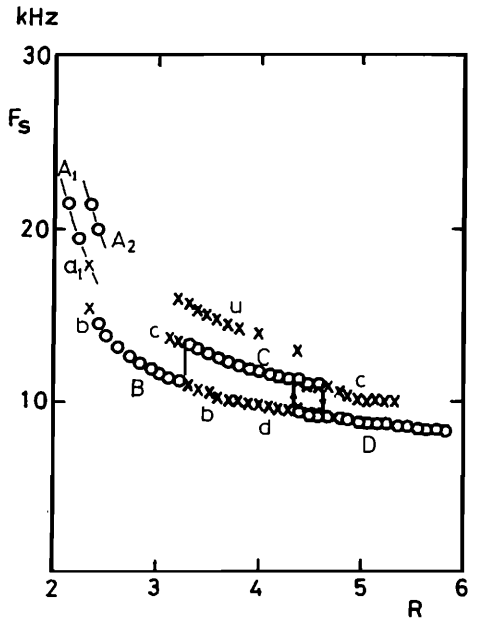

FIG. 2. Frequencies of screech tones at the fixed microphone for the circular jet as a function of pressure ratio. Open data points indicate dominant tones, crosses indicate secondary tones.

The crosses mark *secondary* tones that exceed the broadband noise by 5–10 dB, and these continuous parts are labeled with the lower case of the letters of the dominant tone of which they appear to be a continuation, there being one region where b and d are equally applicable. There is also another secondary tone labeled u, still unidentified.

Tones that are thought to be exact harmonics of dominant tones are not shown since to date there is no reason to think that these have any special significance. Somewhat scattered tones less than 5 dB above the broadband noise are not shown: they lack any distinctive pattern.

The spectra typically resemble those shown in Fig. 3; the pair shown display the hysteresis occurring around the pressure ratio of $R = 4.48$. These also show another interesting feature, namely the pronounced dip in the level of the broadband noise spectrum on the *lower* frequency side of the strong discrete tone. This occurs consistently in the case of mode D and the higher frequency part of mode C, say for pressure ratios greater than about 3.7, but not otherwise.

The results for the dominant tones are clearly essentially the same as found originally by Powell (1953b), except that A_2, first reported by Davies and Oldfield (1962), now appears. In this region it was originally reported (Powell, 1953c) that "no discrete frequency" exists: now it is apparent from Fig. 2 that two strong dominant tones (A_2 and B) occur at the same pressure ratio, but the oscillation switches rapidly between them It is now realized that the original frequency matching method must fail since while "...the motion is very confused, although the amplitudes are still large..." the proper stricter interpretation appears to be that "no *single* discrete frequency exists" here. On the other hand, both Merle (1956) and Davies and Oldfield (1962) did report this stage A_2, implying that the mode B then occurred for relatively little, or for none of the time.

The secondary tones are of interest in that they are present adjacent to all the jumps from one mode to another (with the possible exception of the jumps between the A_2 and B modes, where either mode is dominant). Merle was the first to detect what are now called secondary tones. She found that the secondary tone b (or d) occurred simultaneously with the dominant C tone as found here, but she did not find the secondary c tones nor the brief a_1; on the other hand she did report an extensive a_2 that extended to the frequency where the dominant C tone commenced. The secondary tone labeled u in Fig. 2 may be a similar extension of a_2, but in the current experiments the tone is weak and, lacking any convincing evidence of continuity with a_2, must be considered as unidentified.

B. Schlieren photographs

Schlieren photographs with an exposure of 1 μs were taken to display the jet configuration and possibly the associated sound field for each of the dominant modes, as shown in Fig. 4. The knife edge of the system was at right angles to the jet axis, and such that positive density gradients in the jet direction appear as regions of additional illumination, and negative gradients of reduced illumination. Hence density (pressure) gradients normal to the jet direction will not be recorded.

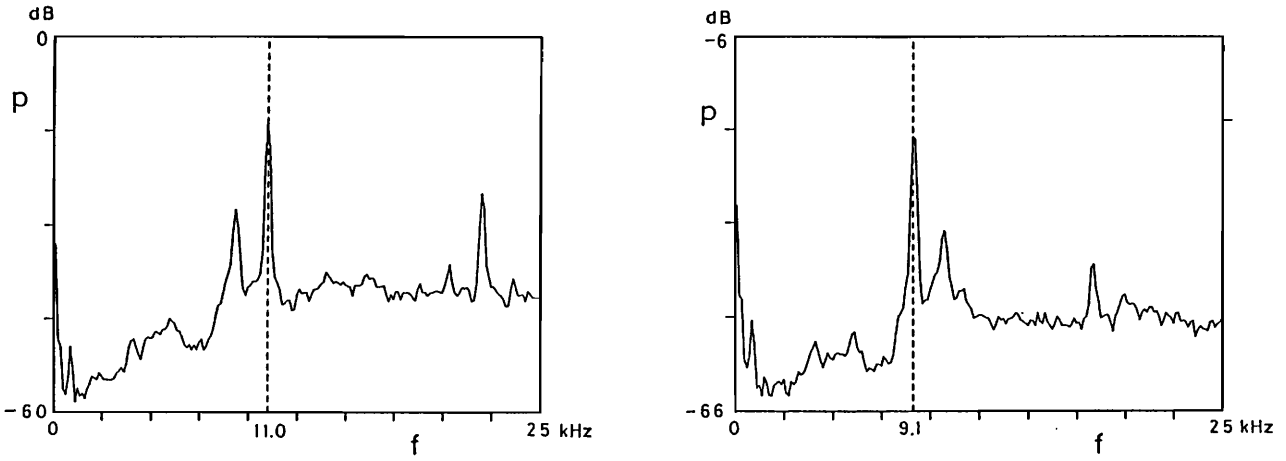

FIG. 3. Typical form of sound pressure level spectra. This pair illustrate the hysteresis occuring at pressure ratio $R = 4.48$, for the pressure increasing on the left with C tone at 11.00 kHz, pressure decreasing on the right with D tone at 9.125 kHz. The high level at and near zero frequency is an artifact.

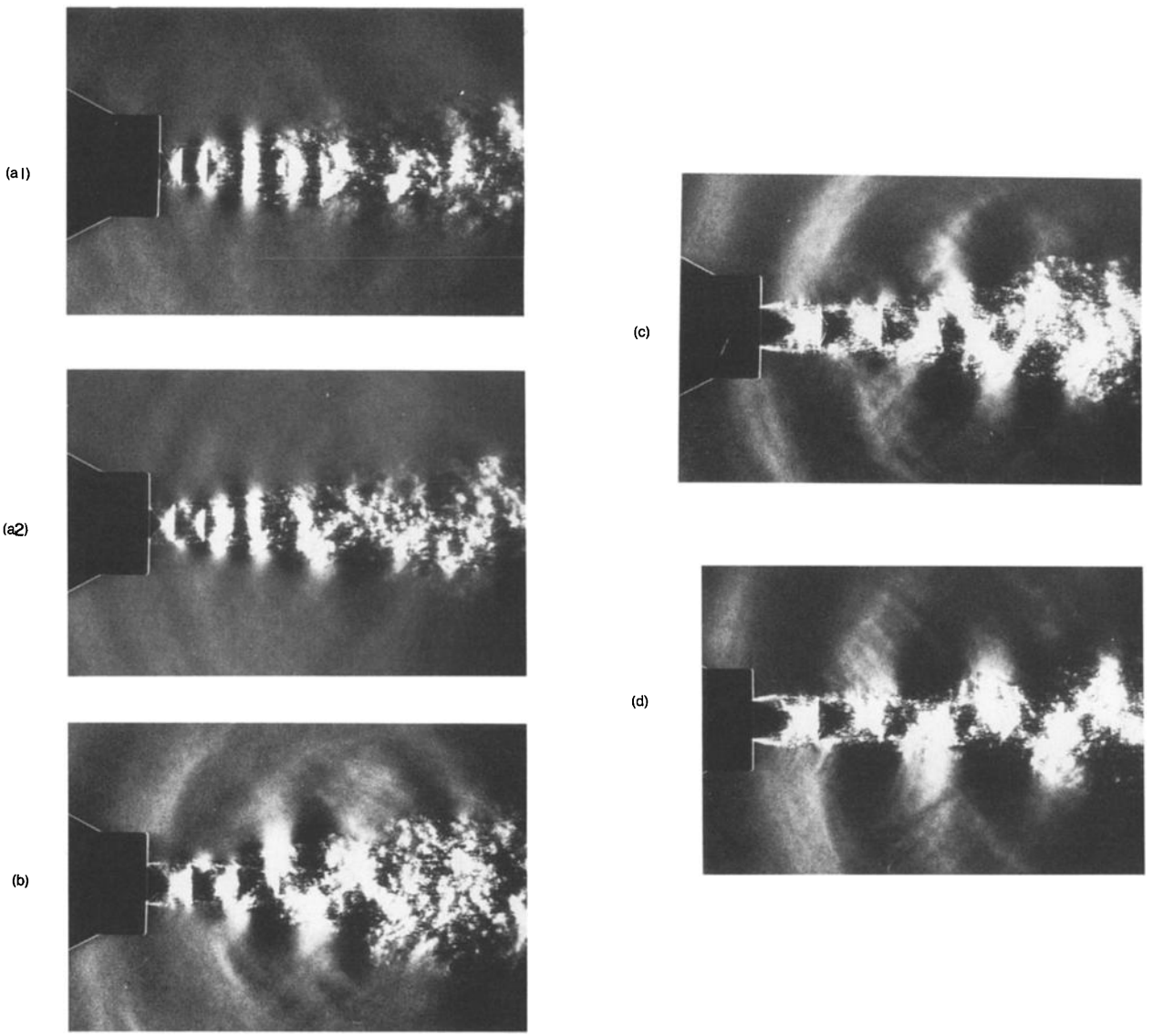

FIG. 4. Schlieren photographs of the jet oscillating in each mode. From top to bottom: (a1) mode A_1 at pressure ratio $R = 2.26$; (a2) A_2 at $R = 2.35$; (b) B at $R = 2.93$; (c) C at $R = 3.90$, and (d) D at $R = 4.87$.

Certain features are common to all the photographs. The roughly periodic structure characteristic of undisturbed choked jets is prominent in all cases, the cell length increasing with pressure ratio. The first cell or two are clearly defined, but further downstream the cells become less and less distinct as the flow becomes dominated by large disturbances and turbulence.

The disturbances in the "ambient" fluid caused by the growing instability waves ("large scale structures") in the jet being convected at high subsonic Mach numbers are very prominent, their alternating density (pressure) gradients in the downstream direction sometimes being visible as far as about one diameter into the "ambient" fluid external to the jet. Because of this characteristic, these are called *evanescent waves*, though it must be realized that they are neither strictly sinusoidal nor two-dimensional.

Sound waves are evident in the ambient fluid, particularly prominent in the cases of the *B* and *C* modes, where they are of opposite phase on each side of the jet. In the case of the *A* modes they are less distinct and are symmetrical, like the stream disturbances.

1. Identification of the instability modes

The dominant deformation of the jet in the case of the *A* tones is clearly symmetric about the jet axis, confirming the previous findings of varicose (toroidal) formations, possibly leading to toroidal vortices if enough nonlinear development takes place. These symmetric instability waves appear to have their maximum amplitude at a distance of some 3–5 nozzle diameters from the nozzle. The local wavelength of these waves and the associated evanescent waves appears to increase significantly as they move downstream.

In the case of A_2, however, the vortex "rings" appear to become tilted and at the extreme right side of the photograph the pattern seems more asymmetric than symmetric, with a much increased spacing (wavelength). Note that at this pressure ratio, $R = 2.35$, the spectral analysis showed the presence of the asymmetric (sinuous) secondary *b* tone (as well as a_1).

For the mode *B* the jet deformation is clearly asymmetric, and the acoustic wave fronts are clearly of opposite phase on the two sides of the jet. The amplitude of the jet disturbances are much larger than for the preceding varicose modes, the maximum amplitude occurring at a downstream distance of 4–6 diameters. The jet spreading is greatly enhanced, the largest in this set of photographs, with the visible boundaries reaching a width equal to about four exit diameters at about seven diameters downstream.

The growth of the jet instability for the rather similarly appearing asymmetric mode *C* appears to take longer to develop than in the previous case, maximizing at 6–8 diameters downstream and the final amplitude is perhaps comparable to that of mode *B* before the pattern is lost in the general turbulence.

The configuration in the last case, *D*, is also clearly asymmetric. The instability wave appears to have the maximum amplitude at roughly 8–10 diameters downstream. The amplitude of the instability wave appears to vary considerably from photograph to photograph in the case of this mode *D*, the one shown being of larger than average amplitude, consistent with Merle's observation (1956) that this mode was not always visible. The reason for this distinctive, and initially puzzling, characteristic is discussed in the next section.

The jet spread appears to be possibly less than that for the *C* mode, and much less than that for the *B* mode. The undulation of the boundaries of the jet is seen more clearly, outwards in the white regions of the positive axial pressure gradient of the evanescent waves, inwards for the black regions.

It might be supposed that the continuous zigzag form of the disturbance in the case of the *C* mode is more suggestive of a helix than are the alternating patterns in the case of the *B* and *D* modes. However such photographs do not make it possible to discriminate with confidence between sinuous (lateral) oscillations confined to any single plane through the jet axis and helical modes about it. We resolve this ambiguity by recourse to correlation measurements in the sound field, yielding phase relationships, as described in Sec. II C following.

2. Convection speed of the jet instability waves

The convection speed of the stream disturbances is important in jet instability theory and in the feedback theory of the self-induced screech. In the source region the convection speed is important in determining the directionality of the acoustic radiation, while the average value from nozzle to source region figures in determining the number of cycles in the feedback loop. The wavelengths Λ in the source region, as made evident by the evanescent waves, can be measured in the schlieren photographs. As the frequency f is known from the acoustic spectra, the convection speed $U_{con} = \Lambda f$ follows. The wavelength Λ is best estimated by making the measurements on each photograph several times (with some interval of time between making them) and then taking the average value, thus minimizing random measurement error.

The results are shown in Fig. 5. The convection Mach number $M_{con} = U_{con}/c_0$ (c_0 being the *ambient* sound speed) displays an increase from about 0.6 to about 0.8 as the pressure ratio increases to 3.5 or 4, and then levels off, or perhaps decreases somewhat.

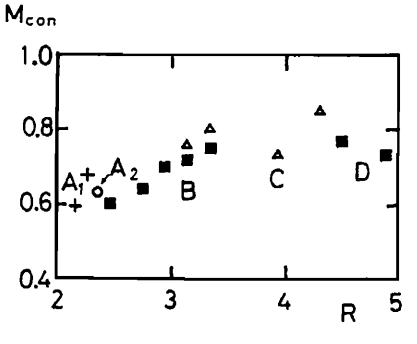

FIG. 5. Convection Mach number $M_{con} = U_{con}/c_0$ of the jet instability waves for the various modes deduced from the measurements of their wavelengths. Legend: +, A_1 mode, ○, A_2 mode, ■, *B* mode, △, *C* mode, and ■, *D* mode.

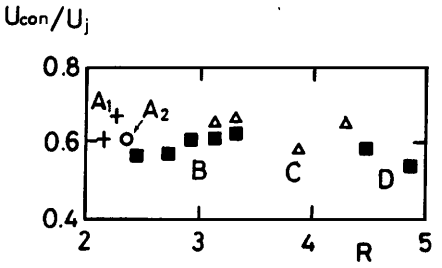

FIG. 6. Convection velocity U_{con} of the jet instability waves versus pressure ratio R for the various modes deduced from the measurements of their wavelengths. Legend: same as Fig. 5.

The mean value for the two stages of the A mode is 0.64. The B mode displays a definite and steady increase, from 0.60 to 0.75, averaging at 0.68. The C mode data suffers most from apparent scatter (even though this is by far the steadiest of all the modes) with an average value of 0.80. The two D mode data points (average value 0.75) might imply a downwards trend.

This parameter M_{con} is important in the feedback theory, but from the point of view of jet instability theory the corresponding parameter of prime interest is U_{con}/U_j, where U_j is the velocity of the choked jet if it were fully (ideally) expanded. If the boundary of the jet is represented by the ideal vortex sheet, then this is the velocity that the jet would have immediately adjacent to that boundary. The result is shown in Fig. 6. While the values of the B mode still increase steadily with increasing pressure ratio, the overall trend is somewhat downwards, with the average value of 0.61 for the 14 data points.

C. Acoustic field—correlation measurements

The method used to determine the phase difference between points in the acoustic field at the two microphones was as follows. The correlogram of the cross correlation of two sinusoidal pressure signals of the same frequency, but with phase difference ψ, as a function of the time delay τ between them is shown in Fig. 7. The time difference ΔT from the origin to the first maximum corresponds to the phase difference ψ, while the periodic time T is given by the time between successive maxima. Hence the phase difference is given by

$$\psi = 2\pi(\Delta T/T).$$

Averaging was done 1024 times and the resolution $\Delta\tau$ was set at 2 μs.

To provide a base line reference, two cases were examined where the mode is unambiguously known and the tones are very powerful, periodic and steady, namely the screech of an unobstructed two-dimensional choked jet and the supersonic hole tone, in which a circular jet interacts with a circular hole in a normal flat plate (Umeda *et al.*, 1988). Schlieren photographs of these are shown in Fig. 8(a) and (b), respectively, the very powerful sound fields of asymmetric and symmetric form being very prominent, the modes being sinuous and varicose, respectively.

The relationship between the phase difference ψ of the sound field at the two microphones and the angle θ between them is shown in Fig. 9(a) and (b). For the symmetrical hole tone shown in Fig. 9(b), the phase difference is found to be close to zero: the data points indicated by circles show the average values, and the error bars show the limit of the scatter of individual measurements, 18 in number. The anticipated values for screech in the sinuous mode are 0 and $\pm\pi$,

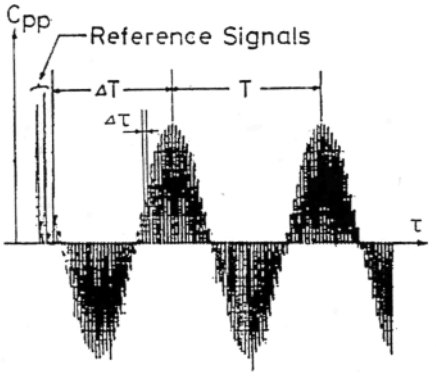

FIG. 7. Correlogram illustrating the phase difference between two sinusoid signals.

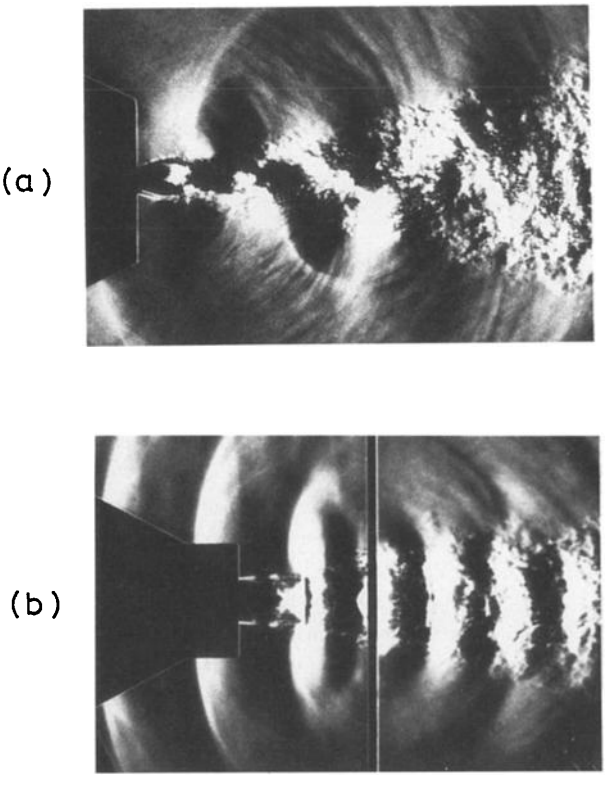

FIG. 8. Schlieren photographs showing (a) asymmetric (sinuous) screech mode for rectangular jet, aspect ratio $b/a = 8.00$, $R = 4.48$. (b) Symmetric hole tone mode, nozzle diameter/hole diameter 2.20, separation distance/nozzle diameter 3.00, pressure ratio $R = 3.90$.

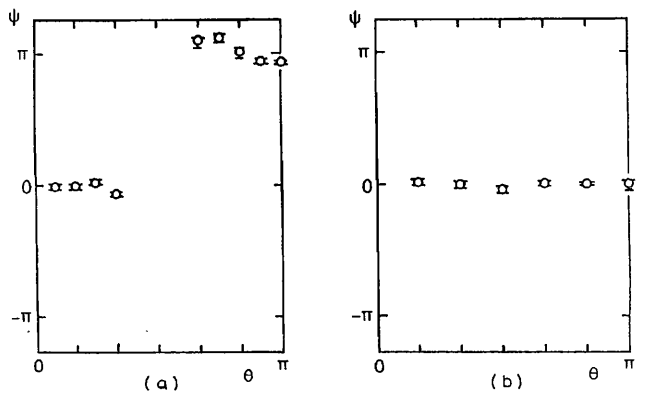

FIG. 9. Variation in phase angle ψ at the moveable and fixed microphones, separated by angle θ, for the situations of Fig. 8, i.e., (a) for the asymmetric mode of screech from a rectangular jet and (b) for the symmetrical hole tone.

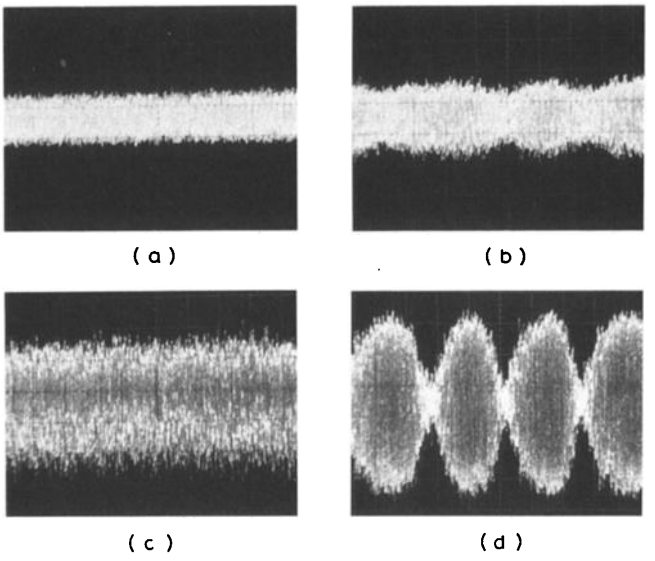

FIG. 10. Oscilloscope traces from the fixed microphone obtained during (a) mode A_2, (b) mode B, (c) mode C, and (d) mode D.

with a discontinuity between them, ideally. The result shown in Fig. 9(a) clearly has the expected character but there are inexplicable minor deviations from the expected values, even though the scatter remains insignificant. But meaningful results could not be obtained when the moveable microphone was at 15° or less from the plane of symmetry. Presumably the signal to noise ratio became inadequate there in the absence of filtering, in the presence of the broad band noise and of possible reflections at the microphones.

It is concluded from this that the method can be useful for determining the phase relationships in the acoustic field, and hence also useful for inferring the mode of instability of the jet; but minor deviations may occur even in the averaged values.

Therefore one may seek to classify the modes as follows: zero phase difference ψ for all θ to indicate a varicose mode, phase differences of 0 and π separated by a gap on the plane of symmetry to indicate a sinuous mode, and phase difference ψ varying as θ from 0 to $\pm\pi$ to indicate a helical mode, the sign being dependent on the sense of rotation.

Simple oscilloscope traces for the acoustic pressure at the fixed microphone for each of the four tones are shown in Fig. 10(a)–(d). The tone A_2 is fairly steady, though its envelope is somewhat ragged on a fine time scale; that of tone B has much more randomness on a larger time scale, with the *envelope* appearing qualitatively like noise, that of tone C is steady apart from a fine scale raggedness like that of the first case, while that of tone D shows a very strong modulation, practically 100% in other (but photographically less reproducible) cases with only minor fine scale raggedness. For the trace shown, the period of the modulation varies, but corresponds to a frequency in the neighborhood of 100 Hz.

In Fig. 11(a)–(d) the values of the phase difference ψ are shown at 15° intervals of the angular microphone separation θ for each of the same five pressure ratios.

For the stages A_1 and A_2 of the A mode in Fig. 11(1a) and (2a), the clustering of the phase difference data about $\psi = 0$ for all angular separations θ supports the photographic evidence that the sound field is symmetric about the axis and that the jet instability mode is varicose. While the average values of the 18 data sets are close to zero, there is noticeably more scatter than for the hole tone of Fig. 9(b).

In Fig. 11(c) for mode C, the linear relationship between the phase difference ψ and the microphone separation θ indicates a helical structure. There are two branches, symmetrical and of opposite sign, indicating that the helix could be of either sense, and in fact the data indicates close to equal probability. Note again that the sense of rotation remained the same during continuous operation of the jet, but was liable to be different when the jet has been turned off and then on again.

Next consider Fig. 11(d) for mode D. There is the clustering about the values $\psi = 0$ and $\psi = \pi$ that one would expect of a sinuous mode, but there is a very marked overlap of the two groups of data, in contrast to the situation in Fig. 9(a) for two-dimensional screech. This is because the 18 data sets are distributed between the two groups, as shown in Fig. 12(b). (The data for the value $\theta = 0$ are inferred since the moveable microphone cannot be made to coincide with the fixed one, while those for $\theta = \pi$ are actual.) There is a clear tendency towards a linear variation of the proportion of points in the two groups, there being a single marked deviation from that. The most logical explanation of these data is that the mode is sinuous, but that its plane of asymmetry is to be found at equally likely angles through the jet axis. But the apparent nearly 100% modulation of the sound pressure at a fixed point, evident in Fig. 10(d), provides a strong argument for considering the oscillation to occur in a single plane that is rotating, perhaps at about 100 revolutions per second. This is also consistent with the marked variation in the amplitude of the jet disturbances as they appear in photograph to photograph in this mode. This point will be taken up again after discussion of the B mode.

Consider Fig. 11(b) for the mode B. Most of the data

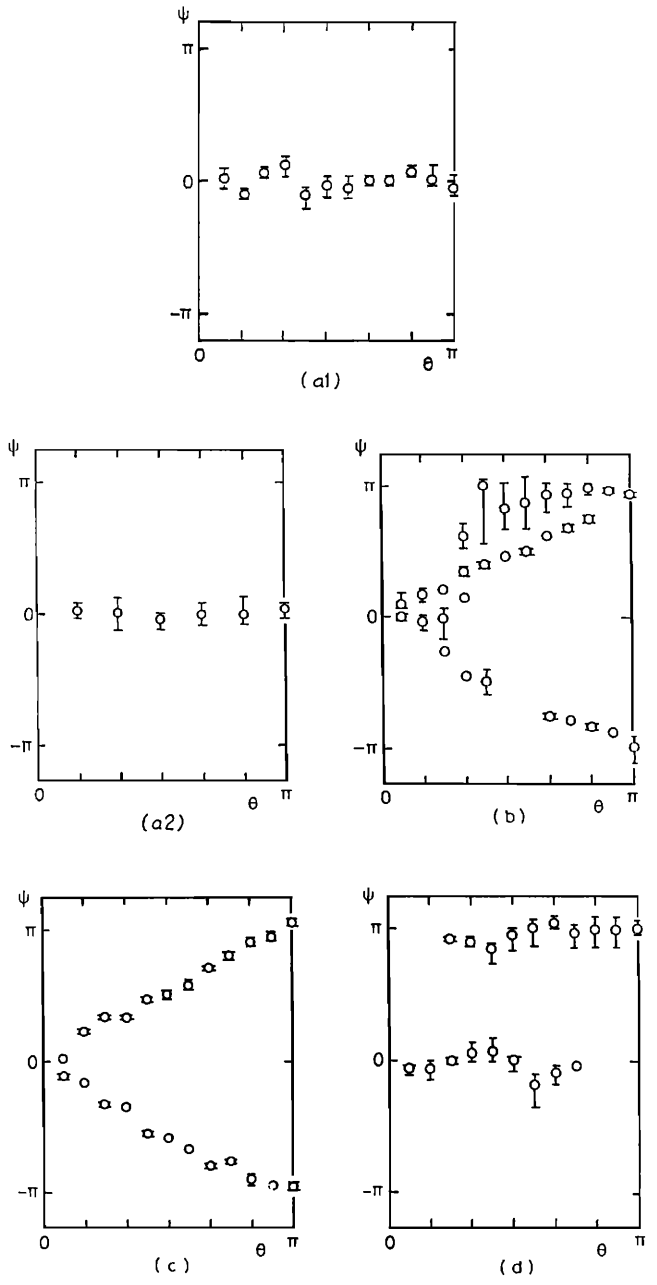

FIG. 11. Variation in phase angle ψ at the moveable and fixed microphones, separated by angle θ, for the screech modes as follows (a1) mode A_1, (a2) mode A_2, (b) mode B, (c) mode C, (d) mode D.

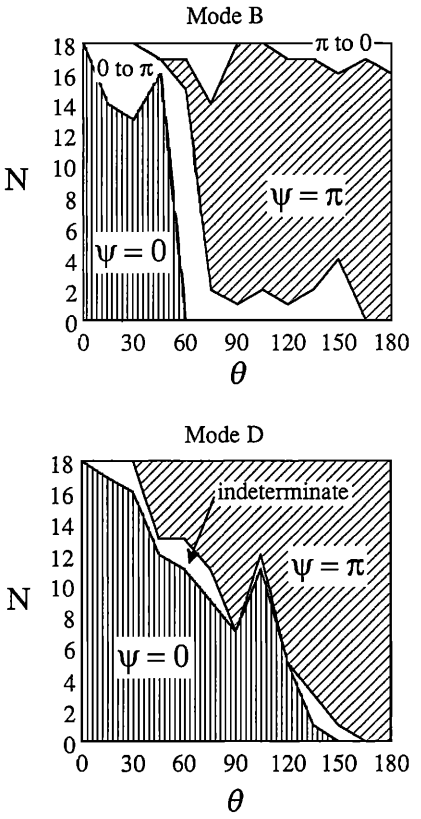

FIG. 12. Distribution of the values of 18 measurements of phase angle ψ at each of the angular separations θ of fixed and moveable microphones for modes B and D.

points cluster about $\psi = 0$ and π, there being a rather wide scatter in the latter case. There are a smaller number of data points which group rather separately to form the pattern of the helical structure already seen in mode C. The distribution of each set of $N = 18$ data points as a function of the separation angle θ is shown in Fig. 12(a). The group marked "$\psi = 0$ to π" is the arm increasing with θ, and that marked "$\psi = \pi$ to 0" is for the downwards sloping arm. There is no systematic overlap of the $\psi = 0$ and π distributions of data points as was evident for the rotating mode D. The pattern is suggestive of the plane of symmetry of the sinuous mode often being fixed at about 60°. This interpretation is probably too simple in view of the relatively large scatter of some of the data points, which is thought to be due to oscillations about planes other than that at 60°. The very irregular envelope of the acoustic pressure signal, shown in Fig. 10(b) supports the notion that the modes flips from one plane to the other spasmodically, or that they occur simultaneously in some rather random way, sometimes appearing to have a helical form. However, though the amplitude at a fixed point varies very irregularly, the frequency remains constant: the spectral peak displays no broadening at all.

Returning to discussion of the rotation of the D mode, the signals from the pair of microphones with 90° separation are shown in Fig. 13, taken at two different times, the moveable microphone being shown in the upper trace and the fixed one in the lower trace. The character of the fluctuations clearly varies from time to time. In general the pattern is complex and may be considered to consist of three characteristic forms. First, in (a) the maxima occur at one of the microphones when the other has a minimum, clearly consistent with a sinuous modes of changing plane of oscillation. In the second case (b) the amplitude of the larger (upper) signal remains nearly constant with time, a small temporary decrease corresponding a larger increase of the lower signal. This is interpreted as the plane of the sinuous oscillation moving temporarily through a small angle from the plane, then returning to it. (In the ideal situation, consider that

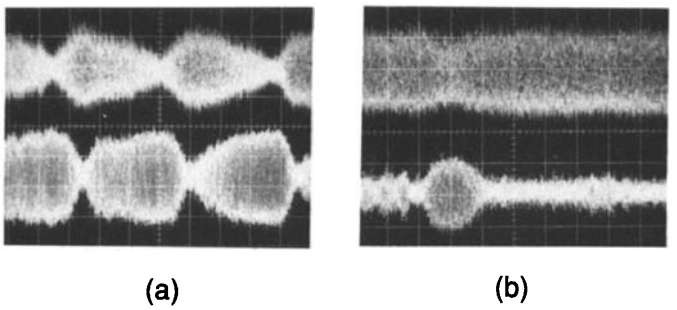

FIG. 13. Oscilloscope traces of the sound pressure fluctuations of mode D at the fixed and the moveable microphone at $\theta = \pi/2$ (lower and upper traces, respectively), at two different times.

small variations of θ hardly change the value of $\cos\theta$ but change the value of $\sin\theta$ significantly.) This may be called a vibration of the plane of oscillation, about a given plane.

In Fig. 14 segments of the oscilloscope traces of Fig. 13(a) are expanded. The first pair (a) correspond to the minimum at the moveable microphone shown in the upper trace in Fig. 13(a), with the corresponding maximum at the fixed microphone (lower trace); see also the interpretive sketch in Fig. 14(f) in which the line marked *a* indicates the situation in this case (a) (the phases are chosen arbitrarily). The second one (b) corresponds to a slightly later time when the two signals have become of comparable strength: they have the same phase as suggested by the line at *b*. The third one, (c), is when the fixed (lower) one has next minimized and the moveable (upper) one is at a maximum, as at *c* in the sketch. The next, (d), is when the signals have again become comparable: the phase relationship has clearly changed to the signals being out of phase. Finally, (e) shows the traces when the amplitudes are the same as in the first case. But as the sketch makes clear, there is a difference in that the phase change across the minimum is reversed. These data are considered to provide strong supporting evidence that the sinuous mode rotates, the phase at a given microphone reversing as the plane of asymmetry passes it.

Sometimes the plane of oscillation undergoes sustained rotation, as indicated in Fig. 15(a), where the rotation speed noticeably increases, and sometimes the dwell, as in Fig. 13(b) is for a relatively long period. Sometimes the motion changes suddenly from one form to another, as shown in Fig. 15(b).

The corresponding variation of the cross-correlation coefficients (time delay $\tau = 0$, $\theta = \pi/2$ still) with time are shown in Fig. 16. As we would now expect, in case (a) of Fig. 13, shown in Fig. 16(a), the coefficient varies between ± 0.5, the distance between the maxima varying irregularly (and there is a noticeable inexplicable asymmetry about the abscissa), while in Fig. 16(b), corresponding to Fig. 13(b) the coefficient is close to zero. Finally, for case (c) the coefficient again varies between ± 0.5 with the maxima becoming closer together as the rate of modulation of the signals of Fig. 15(a) become closer, i.e., as the rate of rotation increases to about 90 Hz. The asymmetry noted for case (a) is absent during the rotational phase.

Thus it appears that, unlike the *B* mode, the sinuous oscillation of mode *D* takes place in a single plane that rotates about the axis in an irregular manner. The three examples given show that it may dwell for some time at a fixed position or rotate at a variable rate for few or many revolu-

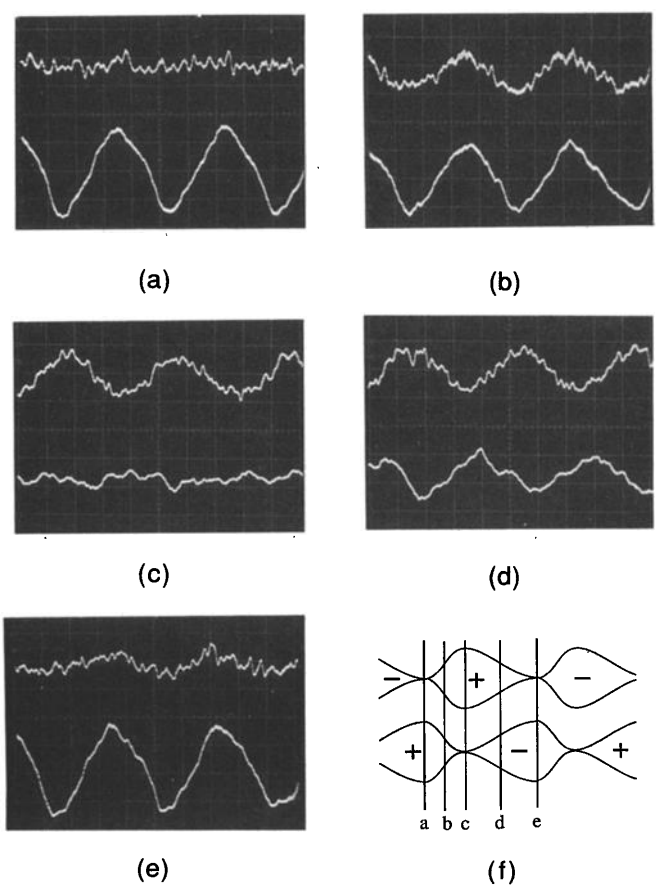

FIG. 14. Expanded oscilloscope traces for the case (a) of Fig. 13. Figure 14(f) indicates the location of the five sets of traces, (a)–(e).

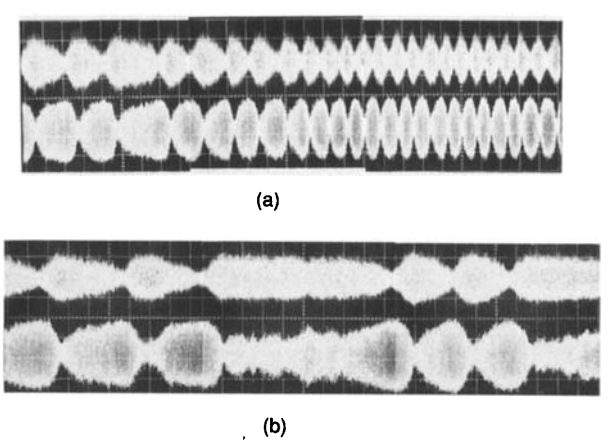

FIG. 15. Oscilloscope traces for mode *D* showing (a) a sustained rotation and (b) erratic motion of the plane of oscillation.

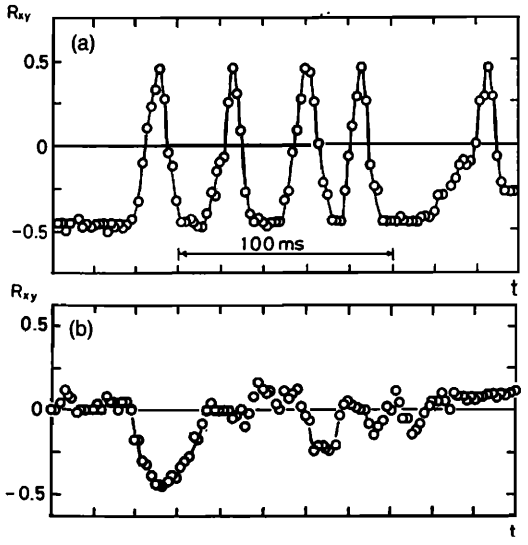

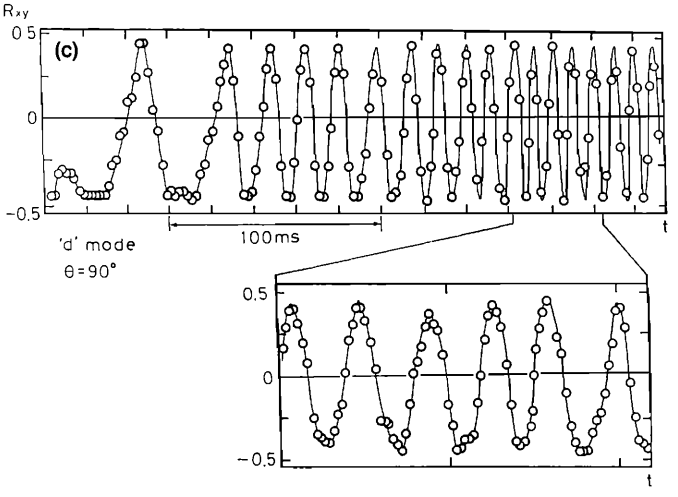

FIG. 16. Variation of the cross correlation with time in the sound field for the *D*: (a) corresponding to Fig. 13(a), (b) corresponding to Fig. 13(b), and (c) corresponding to Fig. 15(a).

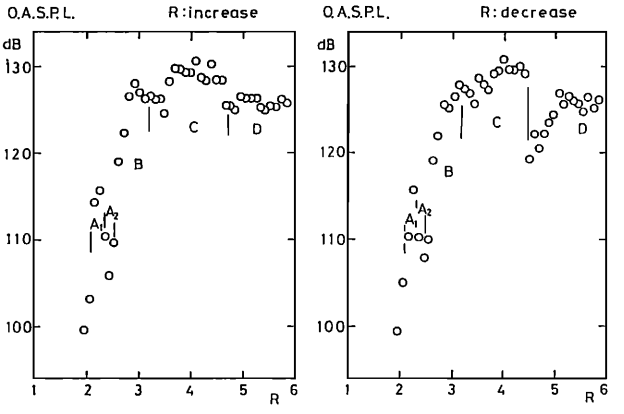

FIG. 17. Overall sound pressure levels in the near field, *re*: 20 μPa.

tions. For example, it has been observed to rotate rather slowly, say the equivalent of 13 Hz, and to rather smoothly accelerate up to about 90 Hz.

The reason for this erratic behavior of the plane of oscillation is not known. It may be due, in part, to the irregular component of the motion of the jet in the downstream part of the sound generating region and also may be due to unsteady initial swirl in the jet as suggested previously (Powell, 1953b), as would apply to the mode *B* as well. The reason for the different behavior of the ostensibly similar sinuous *B* and *D* modes is not apparent.

D. Acoustic field—Sound level measurements

Sound pressure amplitudes were determined at two points in the near acoustic field, using different techniques.

Near-field OASPL data, that approximate to the level of the fundamental, were taken using the fixed microphone and are shown in Fig. 17. The most striking aspect is that the level very rapidly and systematically increases with increasing pressure ratio as the mode passes through stages A_1 and A_2 and enters mode *B* and then the slope suddenly changes with the remainder of the points for mode *B* and for *C* and *D* clustering around the same level of between 125 and 130 dB. When the pressure ratio is decreasing instead of increasing, the only significant change is the mode *D* levels are noticeable lower than those of the *C* mode as the transition to mode *C* is approached.

The second technique was to take the levels of both the dominating and secondary tones from the spectral measurements using the fixed microphone M_f (see Fig. 1). The results are shown in Fig. 18. To reduce the scatter, these data are averaged for points taken with the pressure ratio increasing and decreasing. Exceptions are the data points for tones *C,c* and *d,D* in the hysteretic range where points for the pressure increasing and decreasing are shown individually.

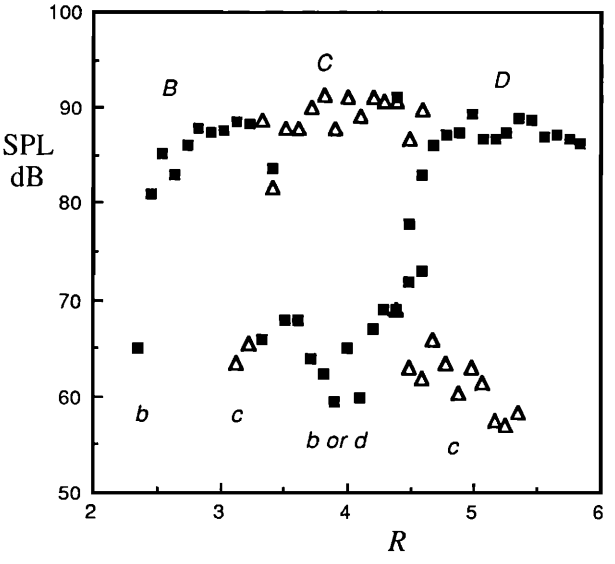

FIG. 18. Sound pressure level of dominant and secondary tones, arbitrary datum.

The tendency noted earlier for the dominant tone data to cluster about a constant sound pressure level is very clear.

The secondary tones exhibit the same tendency, but with more scatter, at a level averaging about 25 dB lower, falling somewhat with increasing pressure ratio.

The few data falling between these two general levels are all associated with the transition from one mode to another, noticeably so in the hysteretic region.

III. DISCUSSION

The instability modes of the jet are evidently any one of the three basic forms, varicose (axisymmetric, toroidal), sinuous (lateral) or helical, and the motion changes suddenly from one form to another as the pressure ratio is changed. The resultant acoustic field naturally has the corresponding form, i.e., axially symmetric, phased oppositely in the plane of the maxima and helical.

A. Varicose modes *A*

As the pressure ratio is increased, the varicose mode A_1 is the first to appear; it is followed by another stage of this mode, A_2. The reason for the difference in frequency of these two stages of the same mode is presumably due to there being a different number of wavelengths in the feedback loop between the effective center (the "centroid") of the stationary sources and the nozzle. That is, if $N+p$ (where N is an integer and $p<1$) is the number of cycles in the loop, then N changes to an adjacent integer. It has been argued that such jumps in frequency occur for the same reason as for edge tones: as the wavelength lengthens (in sympathy with the increasing cell length) at some point it results in a some particular reduced degree of instability of the mode; then a jump upwards in frequency ($N+1$ replacing N) restores the new shorter wavelength of the instability to a greater degree of instability (see Powell, 1961). These instabilities appear to reach their maximum amplitude in the region of 3–5 diameters from the nozzle, where the periodic cell structure is still strong, and so the effective center of the sources can be presumed to lie in this region. In fact, the sound waves visible in the schlieren photograph of Fig. 4(b) for the mode A_2 appear to be centered in a region about five diameters from the nozzle. Then the total number of wavelengths in the feedback loop, $N+p$, appear to have a value of between 7 and 8. (Here $p<1$ is a so-far undetermined phase relationship, expressed as a fraction of a cycle, which cannot be considered *a priori* to be zero, as is sometimes asserted.)

The acoustic radiation of these modes is relatively weak compared to those that follow at higher pressure ratios, but the sound level increases extremely rapidly with increasing pressure ratio.

B. Sinuous mode *B*

The sinuous mode B follows immediately as the pressure ratio increases. In fact, mode B becomes a dominant mode while mode A persists as a dominant mode. Even though this mode is very unsteady, it is much more vigorous, the unstable jet sinuosities reaching maximum amplitude further downstream, say 4–6 diameters. The sound waves appear to emanate from a region about 5 diameters downstream from the nozzle. In this case $N+p$ appears to be about 5.

The resulting angle of spread of the jet is considerably increased over that when the varicose mode occurs. It tends to have a preferred plane of oscillation, but occasionally appears as a helical form. The explanation of this may be made as follows.

In *linear* instability theory, a helical mode may be constructed from two sinuous modes of equal amplitude at right angles to each other and in quadrature. This follows from the simple relationship that

$$\cos\theta\sin(\omega t-kx)+\sin\theta\cos(\omega t-kx)$$
$$=\sin(\theta+\omega t-kx),$$

where k is the wave number (in the downstream direction) of the pair of sinuous jet disturbances represented on the left side of the equation, and of the equivalent single helical disturbance on the right side of the equation. Of course, it may equally well be considered that two helical modes are of the same amplitude but of opposite sense form the sinuous mode, since

$$\sin(\theta+\omega t-kx)+\sin(-\theta+\omega t-kx)$$
$$=2\cos\theta\sin(\omega t-kx).$$

Thus the occasional helical form can be explained if it is assumed that the very unsteady sinuous mode sometimes happens to have the necessary components to appear in the helical form, a seemingly plausible situation.

C. Helical mode *C*

The oscillation in this mode is unambiguously helical, as already reported elsewhere. In these experiments it is about equally likely to occur in either sense, and it is powerful and quite steady. However, the maximum amplitude of the helical instability is not attained until even further downstream, at say 6–8 diameters. The sound radiation appears centered on a region about 6 diameters from the nozzle, the value of $N+p$ being about 5.

The frequency is higher than that of the adjacent B mode, as shown in more detail in Fig. 19. As shown in Fig. 20, the ratio of the frequencies of the C and B modes does *not* remain constant, varying between the maximum of 1.23 to the minimum of 1.14. *If* the relationship between the B and C modes is similar to that between A_1 and A_2, i.e., the principal difference is simply in the value of N, then the most likely ratio of the N's would appear to be $6/5=1.2$ or $7/6=1.17$. As in the other cases, only a rough estimate can be made of the effective source center in Fig. 4(d): it appears to be about 6 diameters downstream, which leads to the ratio of $N+p$ values of roughly 6, which is about what may be expected.

The large amplitude oscillations of the jet extend further downstream than for mode B, so it cannot be considered surprising that the ratio is not constant, although a monotonic variation would appear easier to explain than the rather definite peaked form shown in Fig. 20. The sound intensity, however, is about the same as that for the B mode adjacent to it (see Fig. 18).

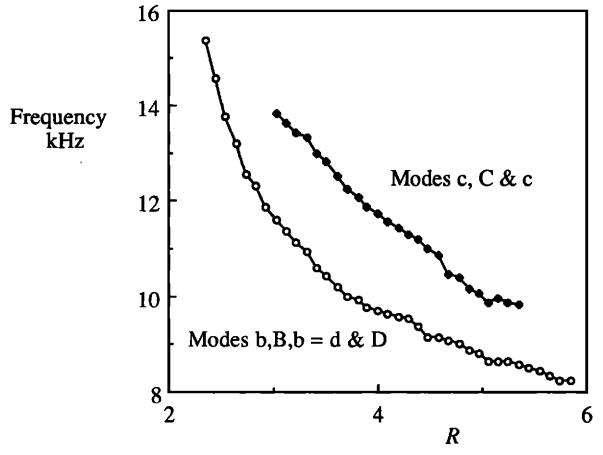

FIG. 19. Frequency of sinuous and helical modes. As the variation of frequency is continuous, no distinction is made between dominant and secondary modes nor the transitions between *B* and *D*.

The amplitude of the helical instabilities of the jet flow becomes very large. In the helical case, one may imagine the instability growing and taking the form of a *continuous* helical vortex, perhaps visible in Fig. 4(d). On the other hand, the sinuous mode appears to develop so as to resemble a Kàrmàn vortex street, but curved around the periphery of the jet like a series of horseshoes. The structures on the two sides of the jet appear to be less continuously connected than in the helical case [the photographs for modes *C* and *D* in Fig. 4(d) and (e), may be compared]. If this is actually the case, then taking two sinuous modes, fully developed, at right angles to each other and in quadrature, and simply superimposing them will clearly *not* form a simple continuous helical vortex. Therefore, as in all the cases observed for modes *B*, *C*, and *D*, the flow disturbances become very large and highly nonlinear, it becomes apparent that it might be desirable to view the fully developed sinuous and helical modes as *essentially* different modes. This might go towards

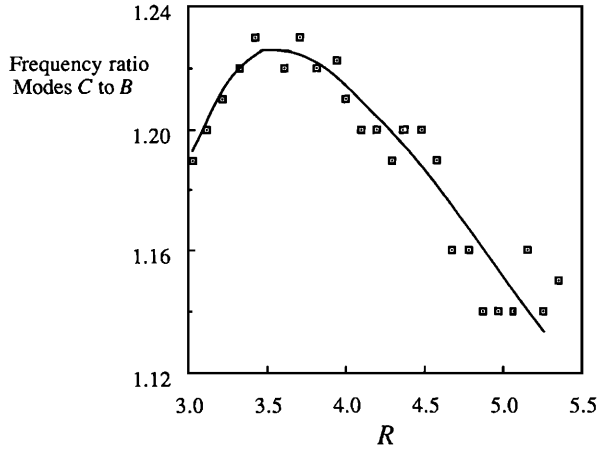

FIG. 20. Ratio of the frequencies of the helical and sinuous modes, one being of dominant strength when the other is of secondary strength.

explaining the varying ratio of the *frequency* of the *C* and *B* modes, as was shown in Fig. 20, even though it has been found that the convection velocities M_{con} are apparently not significantly different.

D. Sinuous mode *D*

This is the last mode to occur with increasing pressure ratio. It is a vigorous mode with about same acoustic intensity as the helical *C* mode, but the degree of instability of the jet is apparently less than for the preceding modes as it reaches its maximum amplitude at perhaps 8–10 diameters downstream. As is clear from Fig. 19, its frequency trend makes a smooth connection with the frequency of the sinuous *B* mode, whether these are dominant or otherwise. Its detailed behavior, however, is quite different to that of the *B* mode. Instead of the sound intensity displaying considerable randomness at a fixed point, the envelope is much smoother in character. The plane of oscillation rotates about the jet axis, sometimes rather steadily but also sometimes in an irregular manner. It perhaps stops at some position for a short time, or seems to vibrate about some mean position, sometimes reversing direction. The most likely cause of this erratic behavior is thought to be initial swirl in the jet itself, but this has not been verified.

E. Nature of the frequency jumps

The progression through modes *A*, *B*, and *C* is accompanied by the maximum amplitude of the stream disturbances (instability modes, large scale structure) moving further and further downstream, the frequency jumps in each case being to higher frequency (except from the varicose mode *A* to the sinuous mode *B*). As discussed earlier in this section, it is easy to explain a jump *upwards* in frequency. The jump to the sinuous mode *D* does not follow this pattern, the jump being *down* to resume the frequency trend of the sinuous mode *B*, although the detailed behavior is quite different.

As the pressure ratio is increased from a low value, screech commences weakly in mode A_1 and rapidly grows in strength. What appears to be some sort of limit cycle is attained near the middle of mode *B* and continues through modes *C* and *D*.

F. Directionality of the effective source

It was originally hypothesized that the self-induced oscillation takes place in the frequency band (strictly, a band of Strouhal number) for which the jet is very unstable, and that within this band, the additional requirement that the radiation from each of the cells, distance *s* apart, must reinforce each other at the nozzle to maximize the feedback (Powell, 1953c). It was later realized that if this frequency is in the region where the degree of jet instability varies rapidly with frequency, then the frequency for overall maximum feedback will likely differ somewhat from that for perfect reinforcement at the nozzle. A measure of the degree of reinforcement at the nozzle is the angle β given by the expression

$$\beta = \cos^{-1}\left(\frac{\lambda}{s} - \frac{1}{M_{con}}\right),$$

since this factor occurs in the expression for the directionality of several sources (Powell, 1953a), and corresponds to the angle that the rather broad maximum makes with the upstream jet direction. Note that this expression does not take into account in any way the helical nature of one mode; one possible effect has been discussed briefly elsewhere (Powell *et al.*, 1990). Here M_{con} and s should be values averaged over the source region. It is not possible to obtain good measurements of this local value of s because of the flow being highly disturbed there, so that of the second cell from the nozzle is used as an approximation, as reported by Umeda *et al.* (1987b). The resulting values of β are shown in Fig. 21. Although there is appreciable scatter, the data points for each mode tend to cluster together, those for mode B being closest to the upstream direction, averaging 16.7°, and those for the C mode being the furthest away, averaging 55.5°. Mode D, the extension of the mode B, has an average value of 36.8°, significantly different.

G. Influence of nozzle lip thickness

The influence of the reflecting surface of the nozzle lip thickness was realized in the early investigations (Powell, 1953d). It has been apparent that there is a definite trend: the larger the lip the greater the "gain" in the feedback loop. This leads to more, or more vigorous, self-induced oscillations, as clearly shown by the experiments of Norum (1983). Careful examination of the spectra did not reveal the extent of secondary oscillations reported all too briefly by Merle (1956) for a very wide lip. Thus this geometric detail is an important one so far as details of the screech tone are concerned.

H. Other possible influence

There is no obvious explanation for the differing behavior of the B and D modes, or for that matter, why mode C is helical in nature and neither B nor D is so. One might suppose that initial conditions at the nozzle would have some influence. Initial conditions concern the state of the boundary layer (laminar or turbulent), the velocity distribution across the nozzle exit plane (depending on the contour of the nozzle contraction), any swirl of the flow, the turbulence level in the flow, or acoustic waves from upstream. If so, then it is likely that different experimental setups will display different detailed behavior since rarely is a significant effort made to minimize or control these factors. The same would be true if the acoustic environment surrounding the jet varies in some significant way from experiment to experiment—for certainly it is known that strong reflections can have a pronounced effect.

I. Secondary modes

While two dominant tones may occur simultaneously, specifically modes A_2 and B at $R = 2.45$, it is much more common that when one mode is dominant, the adjacent one appears simultaneously as a secondary mode at very much reduced strength. Two secondary tones may occur, as may be seen in Fig. 2 at the pressure ratio $R = 2.35$, where the dominant A_2 is accompanied by the secondary tones a_1 and b. As the dominant jet instability mode usually has a very large amplitude, and generally appears to suppress the occurrence of another (inharmonically related) dominant mode, it is somewhat surprising that the latter can survive at all, particularly with the very smooth continuation of the frequency trends evident in Fig. 19.

ACKNOWLEDGMENTS

The first author (A. P.) received support from the Texas Advanced Research Program (Grant No. 003652234-ARP) and from the University of Houston, while the other two authors (Y. U. and R. I.) received support from the Ministry of Education and Culture of Japan (Grant No. (c) 03805007), the Sound Technology Promotion Foundation and Kyoto University, where the experiments were carried out.

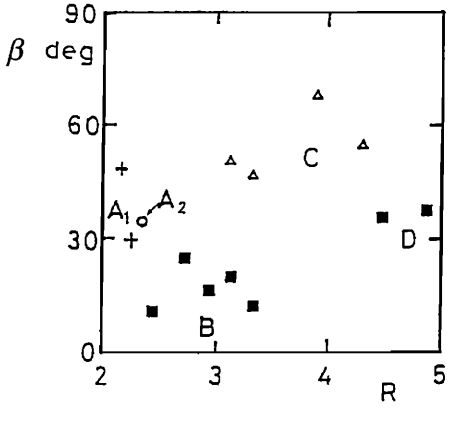

FIG. 21. The angle β as a measure of the closeness of the idealized upstream maximum to the upstream direction. Legend: same as Fig. 5.

Davies, M. G., and Oldfield, D. E. S. (**1962**). "Tones from a choked axisymmetric jet," Acustica **12**(4), 257–277.

Gutmark, E., Schadow, K. C., and Bicker C. J. (**1989**). "Mode switching in supersonic jets," Phys. Fluids A. **1**, 868–873.

Merle, M. (**1956**). "Sur la fréquencies des sondes émises par un jet d'air à grande vitesse," C. R. Acad. Sci. Paris **243**, 490–493.

Norum, T. D. (**1983**). "Screech suppression in supersonic jets," Am. Inst. Aeronaut. Astronaut. J. **21**(2), 235–240.

Powell, A. (**1951**). "A schlieren study of small scale air jets and some noise measurements on two-inch diameter air jets," Aeronaut. Research Council (UK), ARC Paper 14276.

Powell, A. (**1953a**). "On the noise emanating from a two-dimensional jet above the critical pressure," Aeronaut. Q. **4**, 103–120.

Powell, A. (**1953b**). "On edge tones and associated phenomena," Acustica **3**, 233–243.

Powell, A. (**1953c**). "On the mechanism of choked jet noise," Proc. Phys. Soc. London Ser. B **66**, 1039–1056.

Powell, A. (**1953d**). "On the reduction of choked jet noise," Proc. Phys. Soc. London Ser. B **67**, 313–327.

Powell, A. (**1961**). "On the edgetone," J. Acoust. Soc. Am. **33**, 395–409.

Powell, A. (**1962**). "Nature of the feedback mechanism in some fluid flows producing sound," 4th Int. Cong. Acoust. Paper O-22T.

Powell, A. Umeda, Y., and Ishii, R. (**1990**). "The screech of round jets—revisited," Am. Inst. Aeronaut. Astronaut. AIAA Paper 90-3980, October 1990.

Tam, C. K. W., Seiner, J. M., and Yu, J. C. (**1986**). "Proposed relationship between broadband shock associated noise and screech tones," J. Sound Vib. **110**, 309–321.

Tam, C. K. W. (**1988**). "The shock-cell structures and screech tone frequencies of rectangular and non-axisymmetric supersonic jets," J. Sound Vib. **121**, 135–147.

Westley, R., and Wooley, J. H. (**1975**). "The near field sound pressures of a choked jet when operating in the spinning mode," AIAA 2nd Aero-Acoustics Conference, AIAA Paper 75-479.

Umeda, Y., Maeda, H., and Ishii, R. (**1987a**). "Discrete tones generated by the impingement of a high-speed jet on a circular cylinder," Phys. Fluids **30**, 2380–2388.

Umeda, Y., Maeda, H., and Ishii, R. (**1987b**). "Discrete tones generated by the impingement of a high-speed jet on a circular cylinder," Mem. Fac. Eng., Kyoto Univ. **49**, 174–205.

Umeda, Y., Maeda, H., and Ishii, R. (**1988**). "Hole tone generated from almost choked to highly choked jets," AIAA J. **26**, 1036–1043.

Yu, Y. C., and Seiner, J. M. (**1983**). "Near field observations of tones from supersonic jets," AIAA 8th Aeroacoustics Conference, Paper AIAA-83-0706.